0094–1298/99 $8.00 + .00

PHYSICAL ACOUSTICS OF ULTRASOUND-ASSISTED LIPOPLASTY

Keith Weninger, PhD, Carlos Camara, BS, and Seth Putterman, PhD

High-intensity ultrasound capable of cavitating a liquid is an accepted tool in a number of areas of clinical medicine. It is currently used for lithotripsy,[10, 16, 17, 24, 47] cataract extraction with phacoemulsification,[28, 37] surgery (harmonic scalpels),[26, 35] and, of particular interest for this article, ultrasound-assisted lipoplasty (UAL).[1, 11, 18, 48-50] The general usefulness of ultrasound in medicine is probably caused by the ability of the bubbles that it generates to damage[19] tissues by strongly focusing the input acoustic energy to the volume of a cell.

ENERGY FOCUSING IN CAVITATION

When the amplitude of a sound wave in a liquid is above the cavitation threshold of approximately 1 atm, gas bubbles are created. Although the size of these bubbles is much smaller than the wavelength of sound, they nevertheless interact strongly with the sound wave. Figure 1 shows the measured response of an isolated bubble in water to a sound field. When the sound pressure is more negative than the static pressure in the liquid, the bubble grows, slowly absorbing energy from the diffuse sound field.[3, 5, 21, 30, 31] The amount of energy, E_{bubble}, stored in the bubble at the end of its expansion (when its speed is momentarily zero) is given by the mechanical work necessary to expand the bubble against the external laboratory pressure P_0 of approximately 1 atm:

$$E_{bubble} \approx P_0 \frac{4}{3} \pi R^3_{max}$$

where R_{max} is the maximum radius of the bubble. Typically, R_{max} is approximately 50 μm, so that E_{bubble} is approximately 1 erg. Half a cycle later, the net pressure on the bubble is large and compressive, causing a "runaway collapse" of the bubble, first studied theoretically by Rayleigh[29, 32] in 1917 in connection with damage to ship propellers. This runaway collapse is arrested only when the gas inside of the bubble is compressed to the density of a solid. At this moment, when the minimum radius is attained, the acceleration of the bubble wall is approximately 10^{12} g, and the stored energy is delivered to a local-

All research costs were borne by ASERF [Aesthetic Surgery Education and Research Foundation], the National Science Foundation, and the US DOE Division of Engineering Research.

From the Department of Physics, University of California, Los Angeles, California

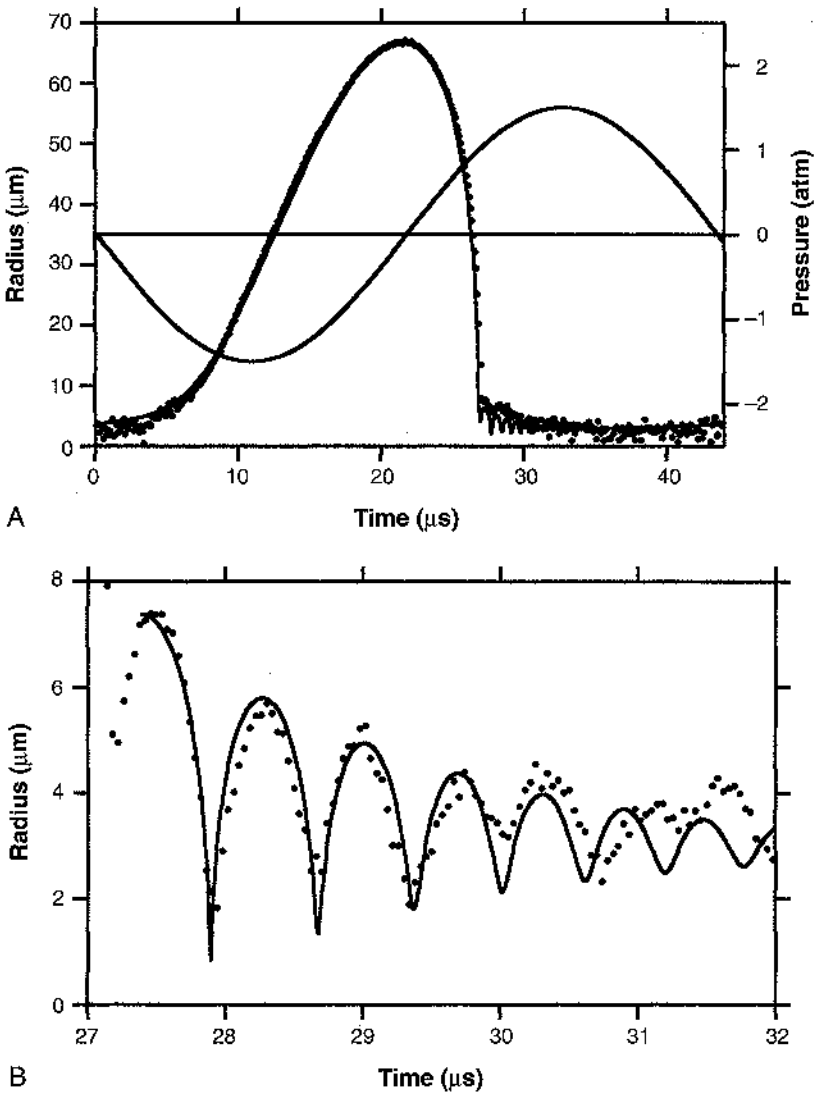

Figure 1. Radius as a function of time for a single acoustically driven gas bubble in water. The dots represent data measured by a light-scattering technique and the solid line is a theoretical prediction of the Rayleigh-Plesset theory for acoustically driven bubbles. The driving acoustic pressure (P_a) responsible for forcing the bubble is also shown. R_0 is the radius of the bubble when P_a is zero. The oscillations of this bubble repeat at 33 kHz. *A*, R_0 = 4 μm, P_a = 1.5 atm. *B*, Detail of the after-ringing of the bubble following the runaway collapse. The maximal radius of this bubble is approximately 65 μm and the minimal, or collapse, radius (not resolved here) is approximately 0.5 μm; so the bubble volume is imploding by a factor of over 1 million. R_0 = 4.0 μm, P_a = 1.5 atm.

ized area near the bubble in a brief subnanosecond burst.[43] Key to the usefulness of cavitation is the remarkable coincidence that size of the region of maximum energy focusing is comparable to the size of a cell; that is, both the minimum bubble radius[5] and the size of a cell are measured in μm.

When spread out over the 4-cm wavelength of a 30-kHz sound wave, an erg is a negligible amount of energy. But when focused on the collapsed volume of a bubble, which is approximately 1 μm in radius, the energy density becomes 10^{11} erg/cm^3, which is equivalent to a stress of 10^5 atm. This is an order of magnitude greater than the stress variation of 0.25 atm required to lyse a micron-sized cell.[27, 36, 38] These huge energy densities are created on a time scale of nanoseconds, leading to power densities of 10^{13} W/cm^3. Though not fully proven, this energy-focusing process is probably responsible for the therapeutic action of ultrasound. The physical acoustic basis for this process is discussed here in more detail.

After the bubble rebounds from its minimum volume, its speed again is zero at the top of its first afterbounce at a radius of approximately 10 μm. Comparing the energy stored in the bubble at this point

$$E_{\text{bubble}} \approx P_0 \frac{4}{3} \pi (10\ \mu\text{m})^3 = 0.004\ \text{erg}$$

to the energy it had absorbed from the sound field during the expansion (1 erg) shows that the bubble collapse returns to the liquid, in a brief instant, 99% of the energy that was taken from the sound field. The energy is delivered to the region via three primary mechanisms (which are not completely independent of each other, as is discussed later): (1) the emission of a flash of broad-band, ultraviolet light, a phenomenon known as *sonoluminescence* (SL)[3, 4, 9, 12]; (2) generation of on outgoing acoustic "shock" wave in the liquid around the bubble[3, 15, 23]; and (3) a focusing of stress, which is promptly converted to heat within a few radii of the minimum bubble size. For medical applications, the localized stress heating is the dominant effect.

The spectral distribution of the light pulse emitted by the collapsing bubble is shown in Figure 2.[3, 13] The presence of large amounts of energy in the ultraviolet range is a general indication that the interior of the bubble is extremely hot. During the collapse of the bubble, the gas inside the bubble is heated through adiabatic compression and possibly imploding shock waves. Matching the light from the hot gas to thermal emission models indicates temperatures in the range 30,000 to 100,000° K. The conversion of the diffuse sound energy into the highly energetic ultraviolet photons is a focusing of energy density spanning 12 orders of magnitude.[4] Despite this tremendous energy density concentration, this light carries away only approximately 10^{-5} of the energy absorbed by the bubble during its expansion. Although not all acoustically driven bubbles emit light (because of a limited range of bubble sizes, acoustic amplitudes, liquid hosts, and gas saturation levels that must be achieved), it is a robust phenomenon occurring in a wide variety of settings. Figure 3 shows spectra of light emitted from bubbles isolated in the center of a sealed container, on the surface of a solid boundary,[42] and generated spontaneously in a Venturi tube flow. By replacing the air that is normally dissolved in the water with xenon gas,[41] we find that light is emitted from bubbles created at the tip of a UAL device operating at therapeutic amplitudes. This light is easily visible to the unaided eye. Photographs of this phenomenon appear in Figure 4, and the spectral distribution of the light in Figure 5. All of the spectra are similar, indicating the presence of a universal effect.

The rapid change in bubble volume during the Rayleigh collapse is a strong source of acoustic radiation. This outgoing acoustic pressure pulse has been experimentally observed for an isolated bubble in water by high-bandwidth needle hydrophones[3] near the bubble and by shadow graph optical techniques.[15] If the time dependence of the bubble radius is given by $R(t)$, and ρ is the ambient density of the water, then the pressure of the outgoing sound wave is proportional to the second derivative of the volume[20] with respect to time, or:

$$P_{\text{scattered}}(t) = \rho \frac{\partial}{\partial t} (R^2 \dot{R})$$

The overdot indicates a time derivative. For

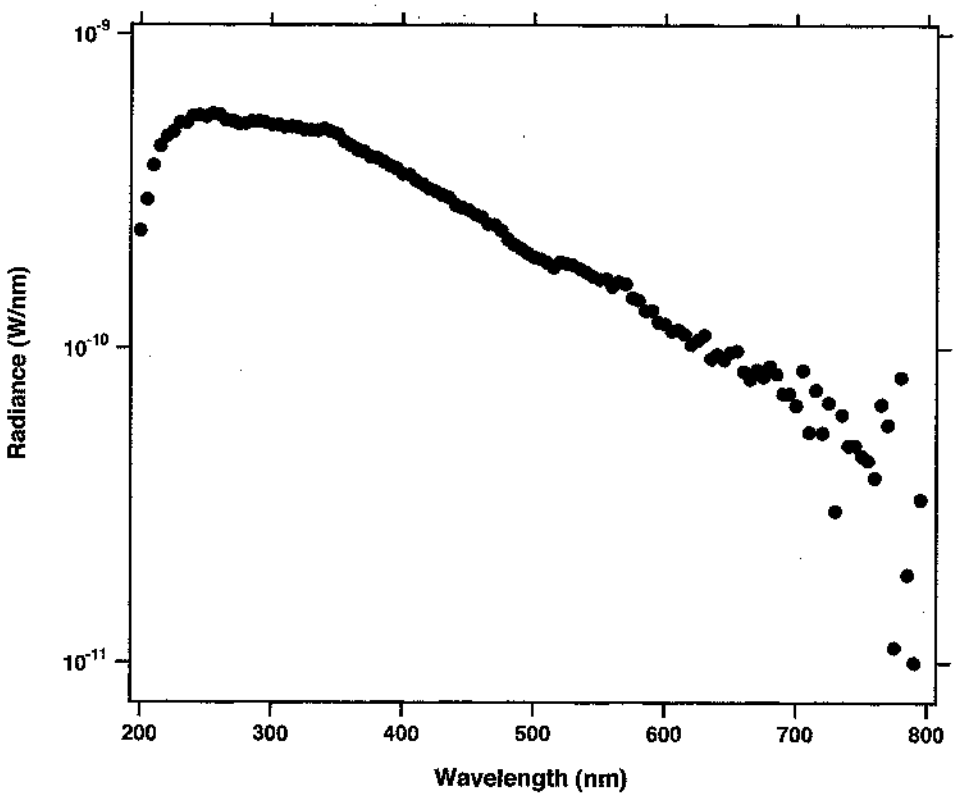

Figure 2. Spectrum of light emitted from a single acoustically driven air bubble in water. The flash of light is emitted during the 50 to 200 picoseconds when the bubble is at its minimal radius. The ultraviolet spectrum indicates that the bubble is hotter than the surface of the sun.

the Rayleigh collapse, a good approximation for the speed of the bubble wall is:

$$\dot{R} = -\sqrt{\frac{2P_0}{3\rho}}\left(\frac{R_{max}}{R}\right)^{3/2}$$

so that we find for the scattered sound amplitude as a function of sound frequency:

$$P_{scattered}(\omega) \propto 1/\omega^{1/5}$$

which means that the bubble converts the pure sinusoidal driving tone into a wide band emission of sound. The power radiated is proportional to the square of the amplitude. Thus, the frequency dependence of acoustic radiation from the collapsing bubble is proportional to $1/\omega^{2/5}$ and extends to at least 3 GHz (based on energy considerations).

Sound waves with frequencies of less than 10 MHz propagate with little attenuation through water and thus leave the region near the bubble. These waves remove approximately 0.1 erg, or 10% of the stored energy in the bubble, and have been seen experimentally as a spherically expanding pressure pulse of a few atmospheres of amplitude and duration of 10 ns to 100 ns approximately 1 mm from the bubble. That tissue damage will result from such a pulse is unlikely.

The sound energy with frequencies of approximately 100 MHz is quickly converted to heat by viscous effects in water within a few microns of the bubble. The enormous accelerations that lead to these highest frequency components of the radiation last only a few nanoseconds. Thus, the cavitation bubble is transducing approximately 85% of the energy absorbed from the sound field, 0.85 erg, into heat within a 10-μm^3 volume of liquid in just a few nanoseconds. This highly localized acoustic stress, which in turn generates a rapid heating near the acoustically driven bubble, probably leads to tissue damage.

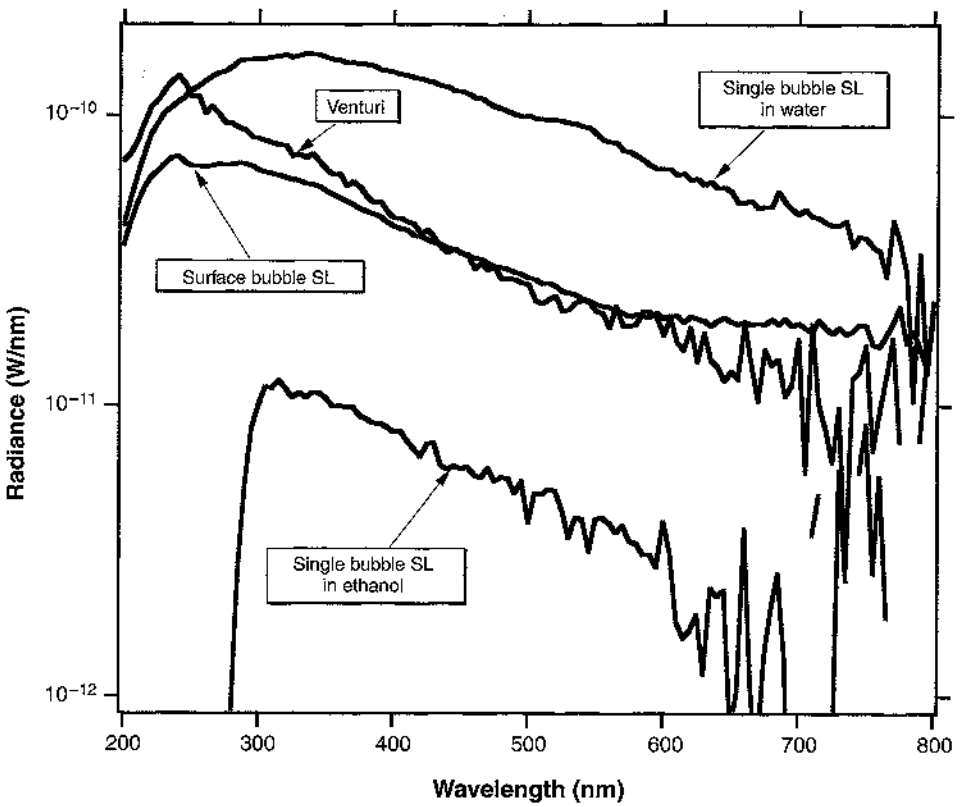

Figure 3. Spectrum of light emitted from xenon bubbles in various settings: Venturi cavitation (50 mm Hg, 28°C), surface-bubble sonoluminescence (SL) (300 mm Hg, 12°C), single-bubble SL in ethanol (325 mm Hg, −12°C), and single bubble SL in water (3 mm Hg, 20°C). The pressure values refer to the partial pressure of xenon dissolved in the liquids. All data are acquired with the same equipment (10 nm full width at half maximum resolution) and are corrected for grating and detector responses. The Venturi data are multiplied by an arbitrary factor for graphical presentation.

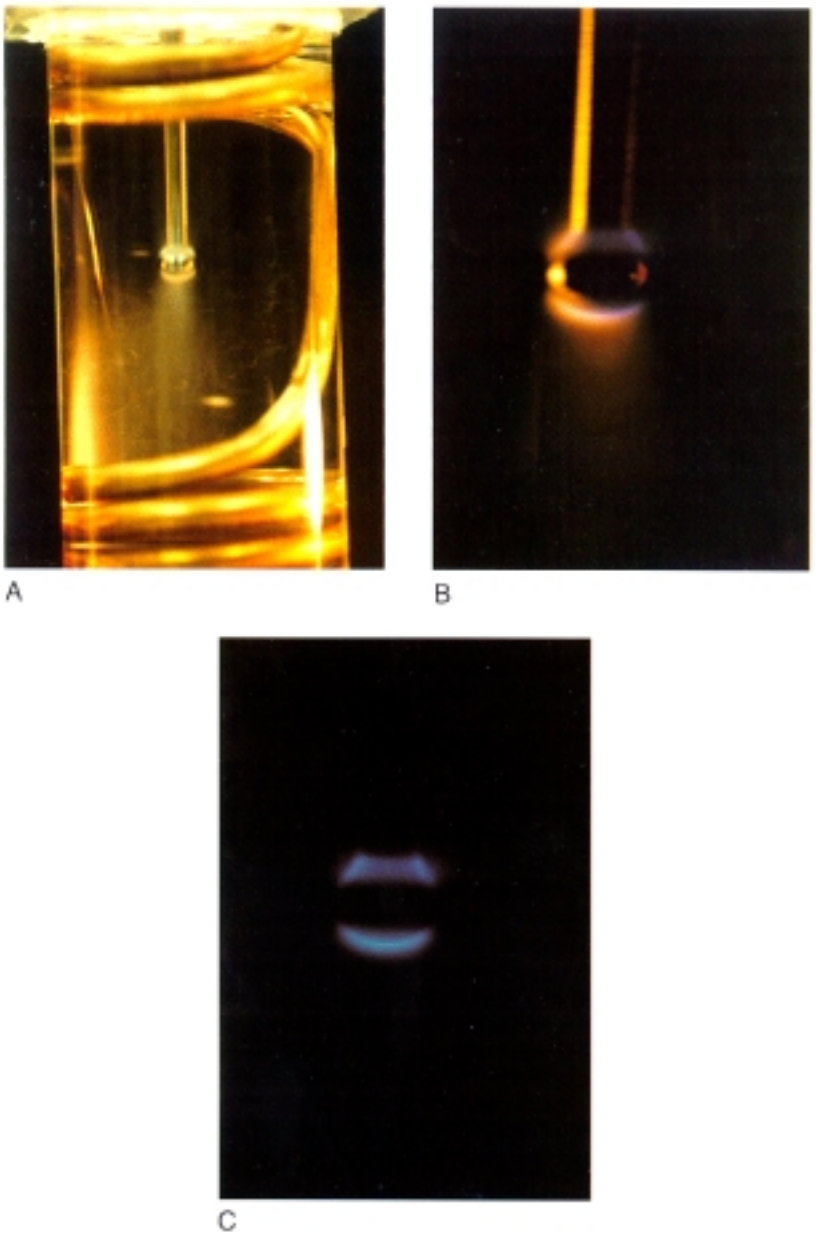

Figure 4. Luminescence from ultrasound assisted lipoplasty (UAL): a dramatic marker for the mechanism of the therapeutic action of ultrasound. *A*, The probe tip oscillating in water with dissolved xenon gas. The copper tubing maintains temperature control. Two types of bubbles can be seen: (1) a beard of bubbles adjacent to the probe surfaces that are most perpendicular to its direction of vibration and (2) bubbles streaming away from the probe tip. *B*, Magnification of the probe showing its beard of bubbles. Taken in dim light, this provides an outline of the tip location. *C*, A 1-minute exposure with no external lighting, showing the sonoluminescence from the 5 mm UAL tip (Mentor) driven at 75% front panel setting power. The water in which the tip is immersed is maintained at 11°C and the naturally dissolved air has been removed and replaced with xenon at approximately 50% saturation. Light originates from a sheath of bubbles that form at the pressure maxima of the dipole sound field set up by the probe. The authors propose that the stress field and heating focused by these bubbles account for the therapeutic action of UAL.

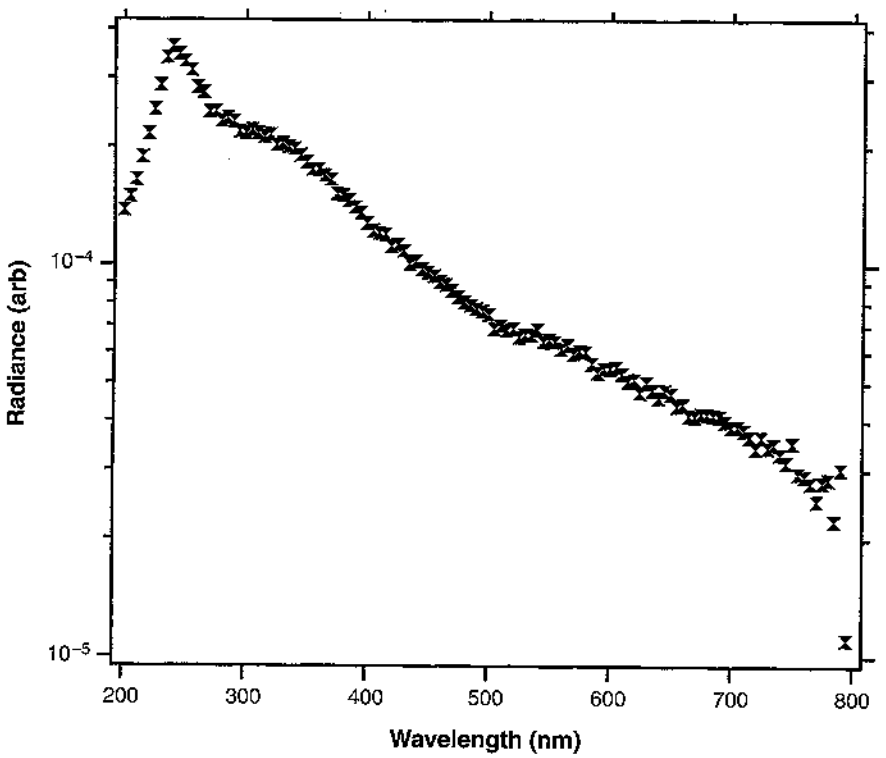

Figure 5. Spectrum of the light emitted by the bubble collapse at the tip of the Mentor 4-mm diameter solid ball ultrasound-assisted lipoplasty device. Front panel power was set to 65% and the water is maintained at 16°C. Data are an average of 16 scans with resolution 10 nm full width at half maximum and have been corrected for the response of the spectrometer and detector. The naturally occurring air was removed from the water, which was then saturated with xenon.

The heating from a single acoustically driven bubble may be compared with the heating caused by the uniform viscous damping of the driving sound wave. Kirchoff's law for the decay of sound gives for the driving sound a direct conversion to heat per acoustic cycle[20] of

$$\Delta Q_k \approx \frac{\omega^2}{u^2}\frac{\zeta}{\rho} T_a \frac{\lambda^3}{8} \rho_0 \langle v^2 \rangle$$

For typical acoustic pressure, amplitudes, P', of 1 atm ($P' = \rho v u$, where v is the velocity amplitude of the sound wave); acoustic wavelength, λ, of 6 cm in water; bulk viscosity, ζ, of 0.1 poise; speed of sound, u, is 1.2×10^5 cm/s; acoustic period, T_a, of 40 μs; the direct viscous attenuation of the driving sound yields a heating of 10^{-5} erg into full volume of $(\lambda/2)^3$, or 10^{-6} erg/cm.[3] The collapse of a single 50-μm bubble, on the other hand, delivers approximately 1 erg to a few microns, or, as mentioned earlier, an energy density of 10^{11} erg/cm^3, a tremendous focusing of heat above and beyond the value attributed to the usual sonic friction.

Figure 6 schematically shows a summary of the energy balance of an acoustically driven bubble. The energy is injected into the system at the ultrasonic frequencies of tens of kHz. In addition to the energy carried away from the bubble as light, sound, and heat from decay of the high-frequency sound, other loss mechanisms include the viscous damping of the collapse of the bubble (accounting for approximately 0.03 E_{bubble}) and the viscous damping of the elastic rebound after the collapse seen as the after-ringing of the bubble (approximately 0.01 E_{bubble}).

PHYSICAL ACOUSTICS OF ULTRASOUND-ASSISTED LIPOPLASTY DEVICES

Ultrasound-assisted lipoplasty is a clinical medical procedure to which the analysis of the energy balance of acoustically driven cavitation bubbles is relevant. The acoustic properties of the Countour Genesis System (Mentor Corporation, Norwell, MA) (27.1 kHz) and the Lysonix 2000 Ultrasonic Surgical System (Lysonix, Inc., Carpinteria, CA) (22.5 kHz) have been characterized with the intent of determining the role of cavitation bubbles in their mechanism of action. Unless otherwise specified, data refer to the Mentor apparatus.

These devices use piezoelectric ceramic transducers inside a handpiece to generate ultrasonic energy that is coupled to the patient

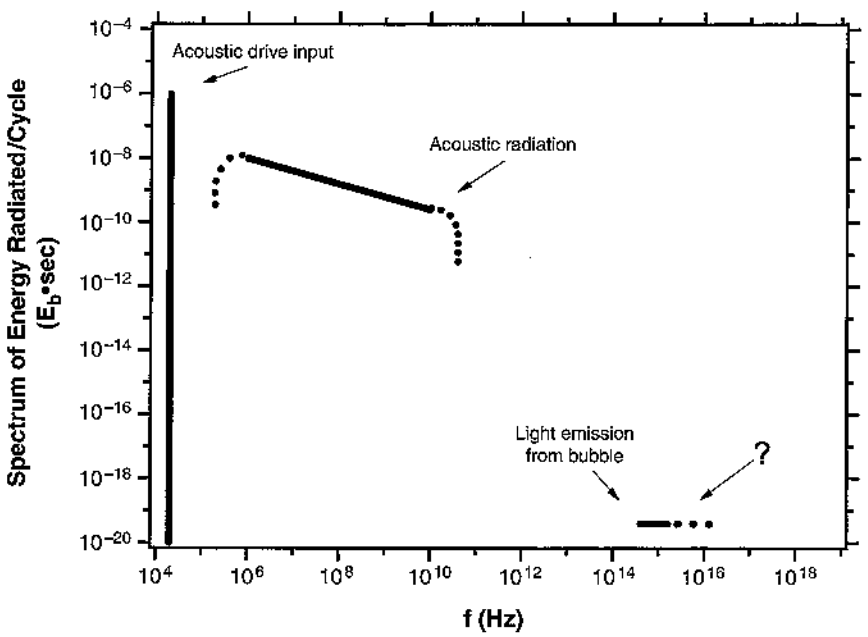

Figure 6. Energy transduction in a collapsing bubble.

through a long (several acoustic wavelengths), titanium probe. Some of the probes are hollow (in which case they are known as *cannulas*) to allow for the removal of soft tissue via suction coincident with the application of ultrasound. The longitudinal vibration of the tip of the probe in a fluid is a dipole source of acoustic radiation. If Δx is the peak displacement amplitude of a sphere of radius R (approximating the probe tip) undergoing harmonic motion, then at a position r (bold denotes vectors measured from the center of the sphere) the deviation of the pressure from ambient caused by the radiated acoustic wave is given as

$$\delta P(\mathbf{r},t) = \rho\omega^2\Delta x \frac{R^3}{r^3}\hat{\mathbf{d}}\cdot\mathbf{r}\frac{(ikr-1)}{(2-2ikR-k^2R^2)}e^{ik(r-R)-i\omega t}$$

where $\hat{\mathbf{d}}$ is a unit vector along the direction of the tip vibration and k is the wave number of the sound wave, given through the dispersion relation $\omega/k = c$, with c being the speed of sound in the medium (1481 m/s for water) and $i = \sqrt{-1}$. The displacement field of the imposed sound field is assumed to vary as $(\Delta x)\exp(-i\omega t)$, where ω is the drive frequency divided by 2π. The electronics driving the transducers use feedback in such a way as to maintain a constant tip displacement amplitude Δx for a given user front panel setting under varying tip-loading conditions. Therefore, the physical acoustic properties of the device are fully specified by determining the tip amplitude and frequency. The authors have measured the tip displacement of these devices using several independent methods: microphone, hydrophone, cavitation threshold, and laser vibrometer.

A microphone (Bruel and Kjaer 4138, Copenhagen) was used to measure the acoustic radiation pressure in air. At 100% drive using the Lysonix device, a pressure amplitude of 1 kPa was measured at a distance of 0.5 cm. Using the appropriate material parameters for air, this indicates a peak-to-peak amplitude of 80 μm.

Using a calibrated hydrophone, the pressure amplitude of the sound radiated from a UAL probe immersed in water as a function of distance from the tip along the direction of vibration was measured (Fig. 7). For direc-

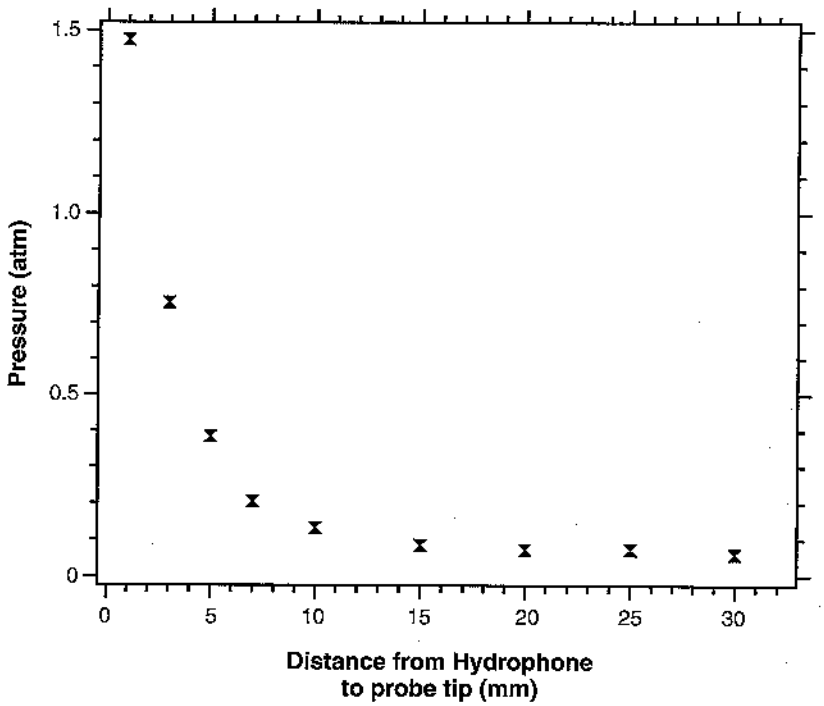

Figure 7. Acoustic pressure amplitude measured by a 1 mm home-made piezoelectric hydrophone (calibrated against a Bruel and Kjaer 8103 hydrophone) as a function of distance from a 4 mm diameter solid probe tip ultrasound-assisted lipoplasty device immersed 1 cm (fixed and the hydrophone was moved) in degassed water and operated at 20% power. Also shown is a $1/r^2$ fit to the data.

tions along the length of the probe, the earlier dipole radiation formula reduces to

$$\delta P(r) \approx \rho\omega^2\Delta x \frac{R^3}{r^2}\left(\frac{1}{2}\right)$$

for $R = 2$ mm and wavelength 5.5 cm and r in the near field range $kr << 1$. From the data in Figure 7, we see that for $r = 5$ mm, we measure a δP of approximately 0.8 atm. This gives a tip displacement, Δx, of 20 μm (40 μm peak to peak) at a 20% user power setting. Calibration by this technique was not possible at higher drive amplitude because cavitation would interfere with the sound.

Consistency of these measurements is seen by a simple consideration of cavitation. In tap water naturally saturated with air, a pressure swing of approximately 1 atm is required to induce cavitation events. With the UAL device tips immersed in ordinary tap water, the authors increased the drive amplitude until the "ping" of individual cavitation events became just detectable. This level is the cavitation threshold and is typically very nearly 1 atm. It was observed at drive levels of approximately 20% for these devices. The front panel power setting was found to be quite linear (by the laser vibrometer method), and, therefore, the authors concluded that 100% power settings will be approximately 5 atm (near the probe) from this measurement technique.

Perhaps the most direct way to measure the motion of the tip of the UAL probes is optically. The authors used a laser Doppler velocemeter (Polytec Vibrometer OFV-302, Waldbronn, Germany) to make noncontact measurements of the tip displacement of the Mentor UAL device both in air and immersed in water. The laser vibrometer measures displacement of a surface by analyzing optical interference between a laser beam reflected from the surface and a reference laser beam. Figure 8 shows the results for various tips in air and in water. The peak measurable amplitude in water was increased by degassing (removing naturally occurring air dissolved in the water) for some data.

The results of all the measurement methods were consistent (at 100% power, tip displacement is 100–200 μm peak to peak), but the laser vibrometer method is the most precise. It shows that for 100% drive, the Mentor device delivers a 60-μm amplitude (120 μm peak to peak) motion at 27.1 kHz, which results in acoustic pressure amplitudes in the range of a few atmospheres (or 2–3 W acoustic power) delivered to the aqueous medium. These uniform pressures are not enough to cause damage to tissue but are just right for the generation and subsequent excitation of cavitation bubbles.

Although the authors have the opinion that lysing is caused by cavitation at the surface of the probe, the acoustic shear layer at the side surfaces of the probe is also strong enough to lyse cells.[44, 45] At a boundary, a source of sound creates a shear motion in addition to the usual, well-known bulk or compressive motion. The shear motion drops to zero amplitude (from the 60-μm value mentioned earlier) over a distance given by the viscous penetration depth:

$$\delta = \left(\frac{2\eta}{\rho\omega}\right)^{1/2}$$

where η, ρ, ω are the fluid viscosity, density, and angular frequency of sound. The penetration depth is approximately 3 μm, much less than the wavelength of sound, which is approximately 6 cm. There is a focusing of stress by the decay of the shear layer given by the factor of merit, λ/δ. The sudden dropoff creates a large surface shear tension:

$$\sigma_a = \omega^{3/2}(\rho\eta)^{1/2}(\Delta x)d_0$$

where Δx, d_0 are the tip displacement amplitude and cell size. Typically, σ_a is approximately 25 erg/cm^2, which is larger than required to lyse cells[26, 36, 38] (most cells have lysis tensions in the range 0.1 erg/cm^2). By determining whether the UAL devices maintain the ability to cut tissue at drive levels significantly lower than that which generates cavitation, the relevance of the shear layer stress could be determined potentially. The authors' device encountered mechanical instabilities that triggered a fault system and deactivated the machine when loaded at such low-drive settings.

Another means of action of strong sound fields is tissue fragmentation.[7, 8] This action is similar to ultrasonic drilling[2] and is probably most relevant to phacoemulsification.

A significant source of complications for UAL is heating from the tip. The authors have

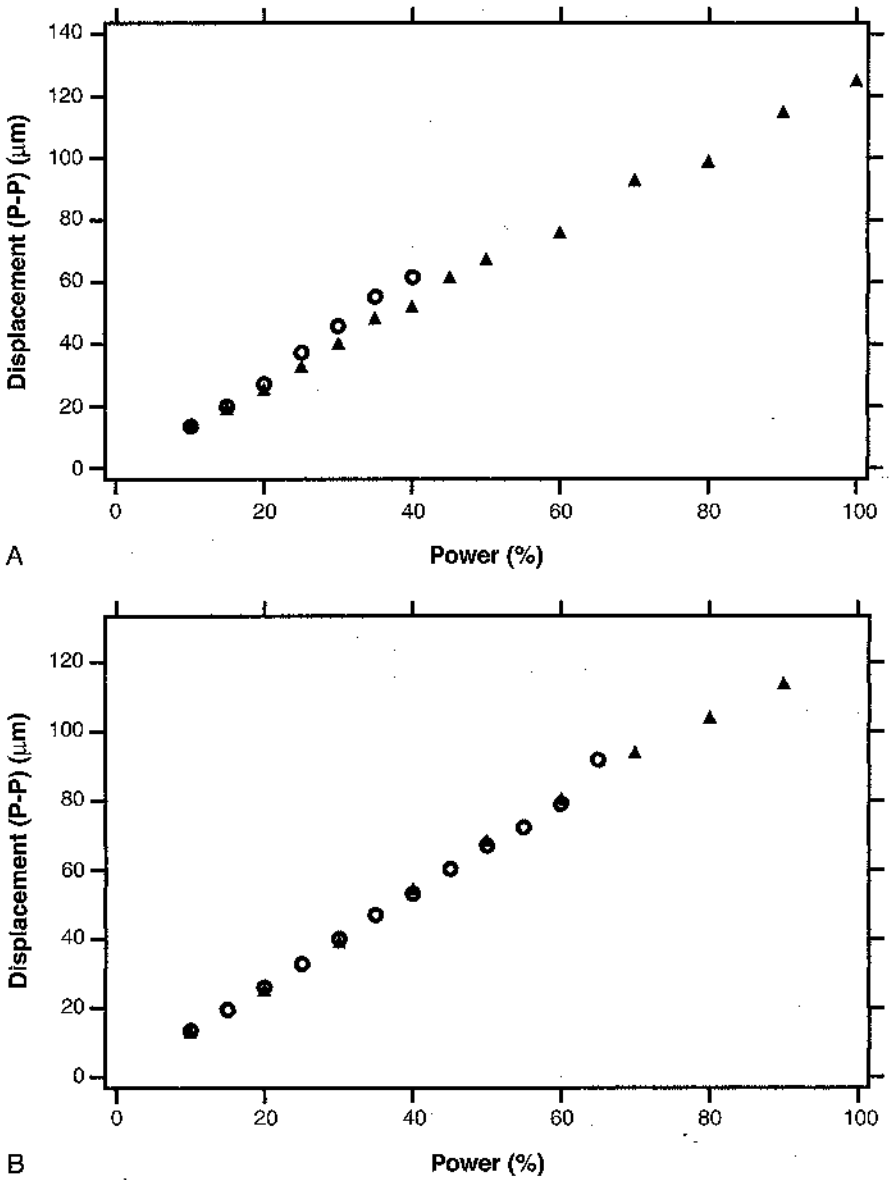

Figure 8. Laser vibrometer measurements of the tip displacement for two different probes on the Mentor ultrasound-assisted lipoplasty device as a function of power setting both in air and immersed in water. Degassing the water allowed higher drive powers to be achieved before cavitation caused the measurement technique to fail. *A,* Four-mm bullet tip 1 cm into water. *B,* Three-mm solid sphere tip 2.5 cm deep. *Triangle* = air; *circle* = water.

used a noncontact, infrared pyrometer to measure the temperature of the tip under various conditions to attempt to learn the source of the heating. At 85% power, in air, the tip was heated to approximately 7°C above ambient temperature and leveled off to a constant temperature after approximately 2 minutes (Fig. 9). The authors then repeated the measurement with the entire handpiece inside a vacuum chamber at 110 mTorr pressure, with the pyrometer viewing the probe tip through a KCl window. In this case, the tip was heated to greater than 15°C in approximately 3 minutes and did not level out. For operation in ambient conditions, air contact cools the probe. Rapid heating occurs when the probe encounters a solid object. To simulate this effect, a 1-mm drop of 5-minute epoxy was applied to the probe tip on the opposite side viewed by the pyrometer and cured approxi-

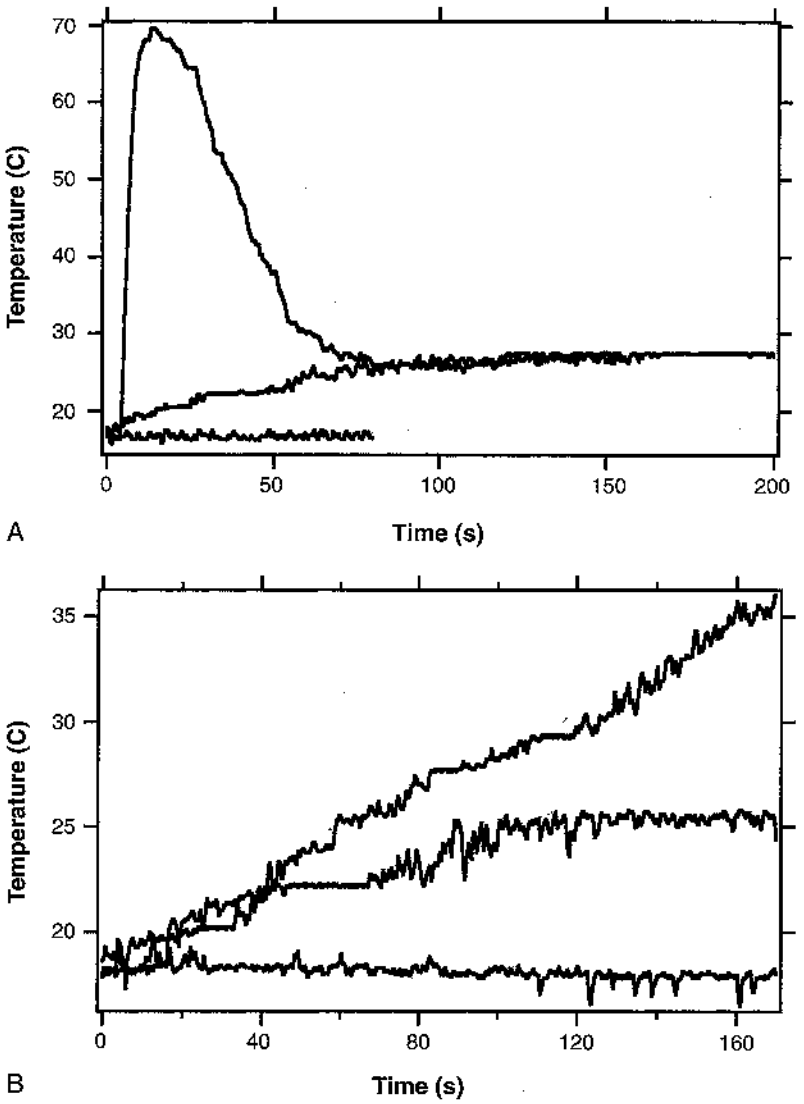

Figure 9. *A* and *B*, Infrared pyrometer measurements of the temperature of a 4-mm diameter bullet tip of an ultrasound-assisted lipoplasty probe (Mentor) under various conditions. *A*, *Top line* = 80% acoustic drive in air, a drop of epoxy applied to the probe; *Middle line* = 90% acoustic drive in air; *bottom line* = ambient conditions. *B*, UAL device inside a vacuum chamber, viewed with infrared pyrometer through a KCl window. *Top line* = 85% drive, 0.1 mm Hg; *Middle line* = 85% drive, 760 mm Hg; *bottom line* = no drive, 760 mm Hg.

mately 10 minutes. Anything more substantial would trip the electronic shutoff circuits. A 50°C temperature increase occurred in approximately 3 seconds, after which the epoxy was flaked off and then the probe cooled until it reached the same steady temperature (7°C above ambient) that was previously measured for operation in air. No tremendous heating occurs as a result of the internal stress of the probe, but the friction with a solid generates great heat. The usual mode of operation for the probe is in water, and so the authors measured the temperature of 13.6 g of water with a thermocouple, while a 4-mm bullet tip was immersed 25 mm and operated at 40% power. In this case, a steady rise of water temperature of approximately 40°C occurred in approximately 3 minutes (Fig. 10). Whether this heating is caused by viscous damping of the shear layer near the probe or the heat transduced by cavitation bubbles is not known.

The cavitation produced by the UAL probes in water generate two types of bubble formation in the vicinity of the probe: (1) on the forward-facing and backward-facing surfaces is a sheath of bubbles and (2) streaming away from the tip of the probe one also finds a distribution of bubbles. To determine which bubbles oscillate at high amplitude, the authors replaced the air dissolved in the water with xenon. For reasons that are not understood, xenon is an extraordinary indicator of strong bubble collapse, emitting visible light under such conditions. Figure 11 shows the intensity of light detected by a photomultiplier tube as a function of user-determined power setting for air-saturated and xenon-saturated water. The light from the xenon water (unlike the air water) is easily visible to the eye (see photographs in Fig. 4). The xenon-saturated water allowed the authors to observe that the bubbles on the forward-facing and backward-facing sides of the tip light

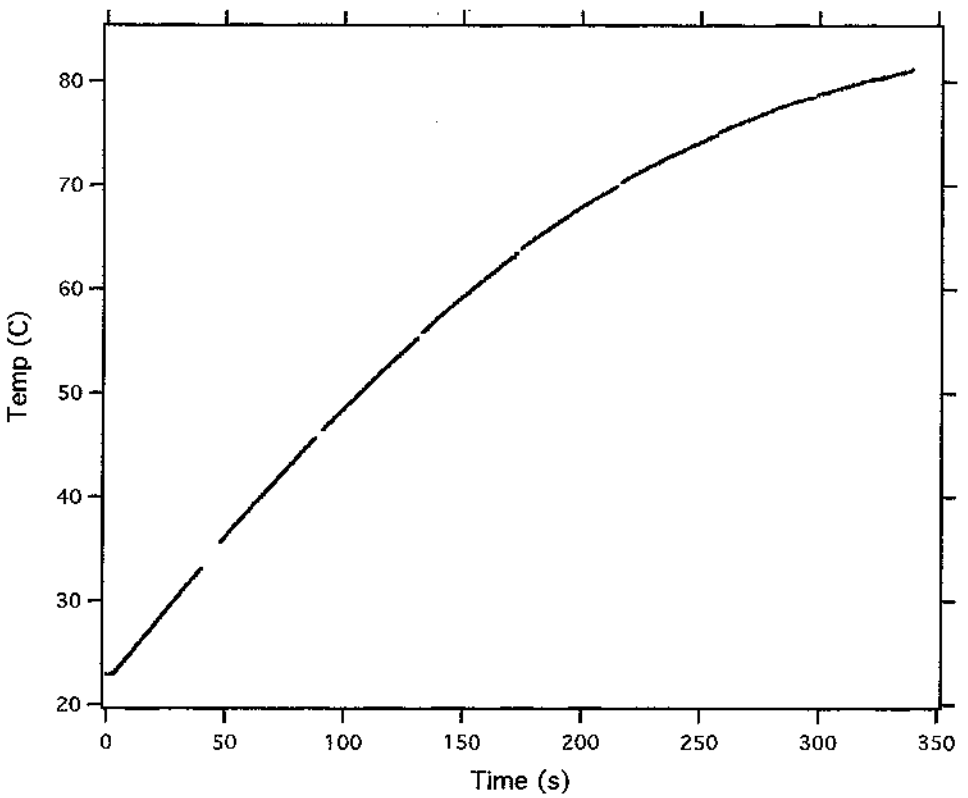

Figure 10. Temperature of 13.6 g of water as a function of time measured with a thermocouple while operating a 4 mm diameter bullet tip immersed 25 mm of an ultrasound-assisted lipoplasty probe (Mentor) at 40% power. At this power level, a full cavitation cloud is created.

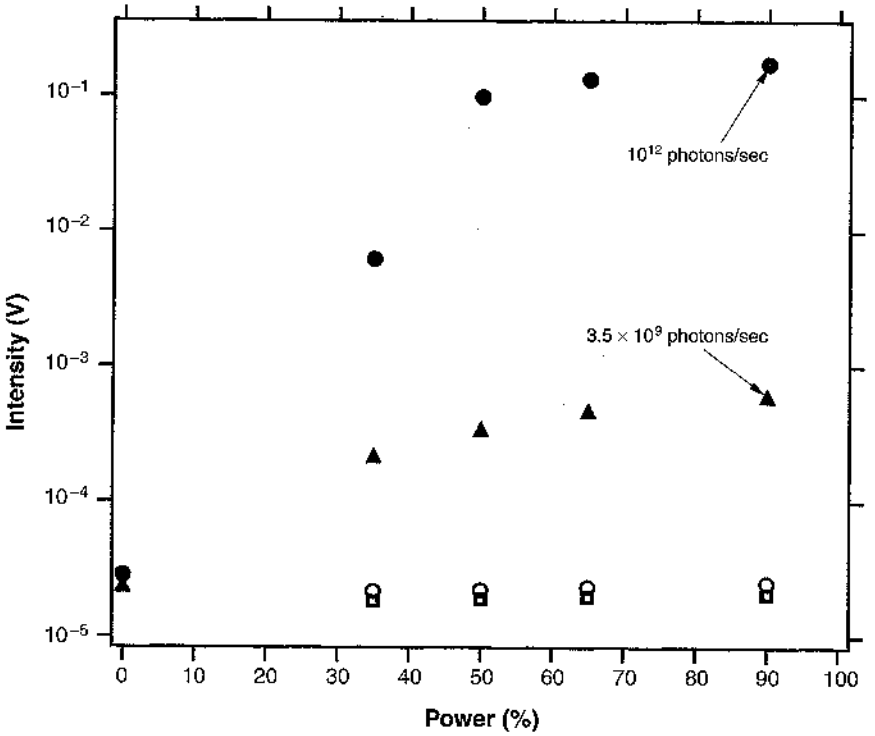

Figure 11. Intensity of light emitted from cavitation at the tip of an ultrasound-assisted lipoplasty probe as a function of power setting for air and xenon-saturated water measured with a photomultiplier tube (PMT) terminated in 10 Kohms. The noise curves are measured by placing a piece of cardboard between the PMT and the probe tip; these measurements agree with the dark current specifications (2nA). The number of photons per second indicated is calculated from specified gain and responsivity of the PMT as well as the solid angle collected. *Solid circle* = xenon-saturated water; *triangle* = air-saturated water; *open circle* = xenon-noise; *square* = air-noise.

up but that the streaming bubbles do not give off light. The authors conclude that the effective cavitation occurs at the tip and that the streaming bubbles do not deliver much stress to the system. Use of the tip to break up fat tissue in commercially available bacon only occurred when contact was made with the tip. The authors saw no damage from the streaming type of bubbles. The next step in this investigation is to make direct measurements of the dynamics of the bubbles driven near the surface of the probe tip.

The spectrum of the light emitted from the water saturated with xenon was measured (see Fig. 5) to be strongly ultraviolet. The light from the air-saturated water (as is more interesting from a clinical application perspective) was too dim to resolve spectrally with the apparatus. (It could be resolved with a gated image–intensified charge coupled device for spectrometer readout.) Nevertheless, the authors could establish that the medically relevant system of air-saturated water did generate light at a level that was down by a factor of 300 from the xenon water. In other SL systems, air and xenon have similar spectra, and one would expect that to be the case here as well. The authors did verify the presence of light with wavelength between 200 nm and 250 nm by using such a bandpass filter between the probe tip and the photomultiplier tube.

CONCLUSION AND SAFETY ISSUES

The acoustic fields generated by the UAL devices create phenomena, such as SL, that are currently under investigation as forefront areas of research in physics. The intensity of SL from tap water that is excited with a UAL device corresponds to a flux of approximately

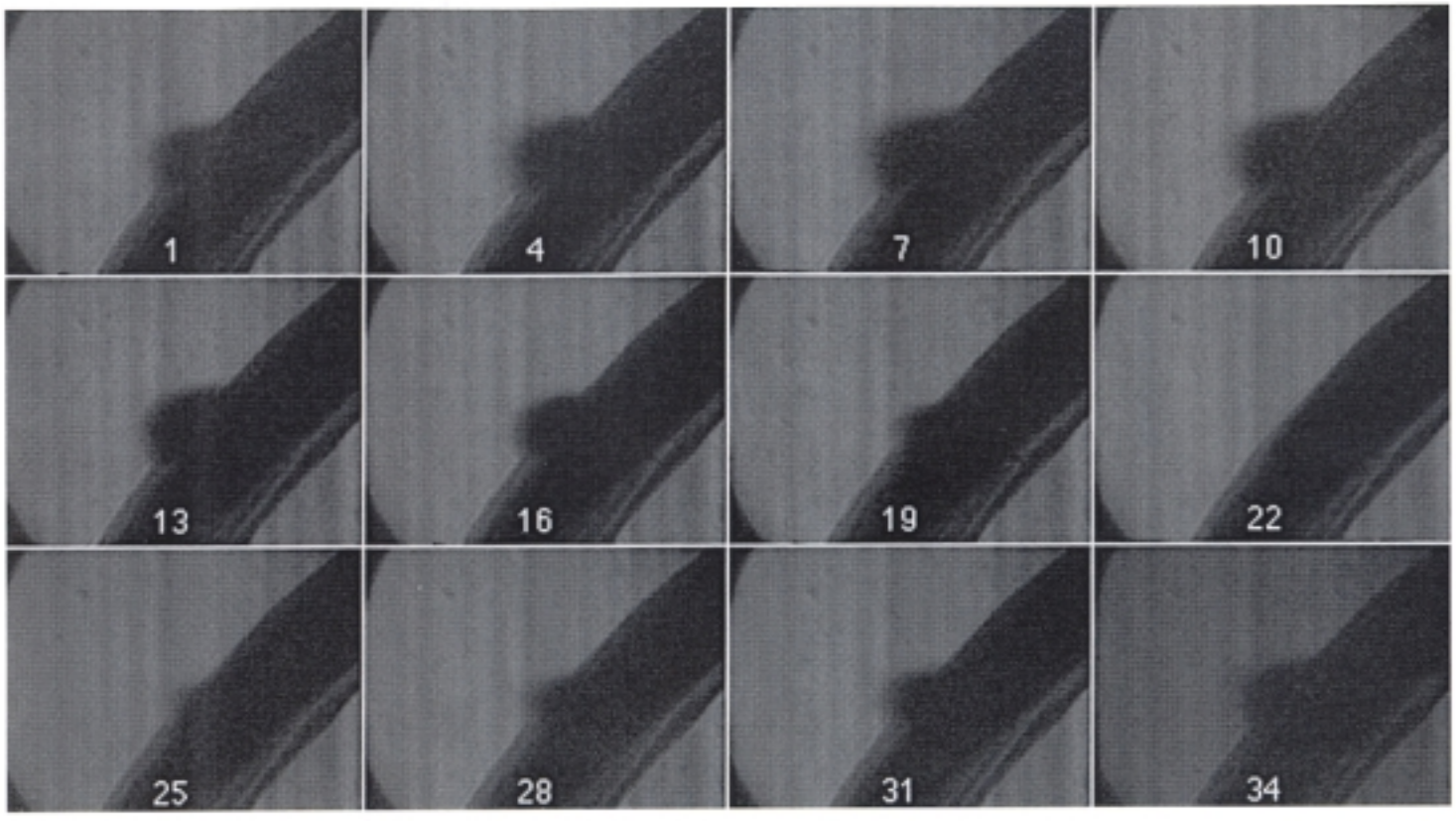

Figure 12. One cycle of the oscillations of a 350 mm Hg acoustically driven, light emitting, hemispheric xenon bubble on the surface of a wire immersed in water. The radius of the bubble is approximately 250 μm. White numbers indicate the time in microseconds. (*From* Weninger KR, Cho H, Hiller RA, et al: Sonoluminescence from an isolated bubble on a solid surface. Physical Review E, The American Physical Society 56(6):6745; with permission.)

3×10^9 photons per second. The photons originate in a thin sheath of bubbles on the forward and backward surfaces of the probe-tip of the UAL device. The authors believe that these bubbles are hemispheric, with the flat side following the surface of the probe. Powerful bubble implosions that maintain hemispheric symmetry have been photographed in similar geometries (Fig. 12).

Let us now consider the relevance of these findings to the issue of the safety of UAL devices.[34, 39] The concern is whether a procedure that uses this device can cause damage to DNA in living cells. Two possible channels have been discussed: (1) x-rays from SL and (2) free radicals. With regard to x-rays, no evidence shows that the SL hot spot also emits x-rays. It has not yet been ruled out, but such a discovery (x-rays from SL) would constitute a tremendously great scientific advance. Such an advance would lead to all sorts of therapeutic uses for sound. To invoke such a dreamed-for discovery as the basis for a safety caution on UAL seems far-fetched.

Free-radical production is, however, the basis for a rational debate about the safety of UAL. The ultraviolet photons produced can interact with water to make peroxide, which, in principle, can cross cell walls to create free radicals and cause DNA damage.[6, 24, 25] The maximum quantities of peroxide that is dealt with in a given 1-hour procedure can be estimated by assuming that each photon creates one peroxide molecule. Thus, a procedure creates approximately 100 picomoles. Does such a potential density of free radicals pose any danger? Many issues come to play here, not the least of which is the absence of a cancer warning on bottles of peroxide. The body has evolved strong defenses against peroxide and the damage it would do. Especially notable are the peroxisomes and the peroxide-neutralizing enzymes that they produce.[22, 33, 40] Experiments in vitro clearly show DNA damage caused by peroxide,[25] but this may be a classic example of the difference between in vitro and in vivo, in which specific feedback loops come into response.

It would be unfortunate if the debate about UAL safety took place at the expense of efforts to define its clear clinical advantages over suction-assisted lipoplasty.[11] And in the wider sense, it would be unfortunate if these issues hindered the development of new applications for ultrasound in medicine.

ACKNOWLEDGMENTS

We thank Mentor and Lysonix for the loan of equipment. We thank M.A. Hamon and Leroy Young, MD, for valuable discussions.

References

1. Adamo C, Mazzocchi M, Rossi A, et al: Ultrasonic liposculturing: Extrapolations from the analysis of in vivo sonicated adipose tissue. Plastic Reconstr Surg 100:220, 1997
2. Babikov OI: Ultrasonics and Its Industrial Applications. New York, Consultants Bureau, 1960
3. Barber BP, Hiller R, Löfstedt R, et al: Defining the unknowns of sonoluminescence. Phys Rep 281:65–143, 1997
4. Barber BP, Putterman SJ: Observation of synchronous picosecond sonoluminescence. Nature 352:318–320, 1991
5. Barber BP, Putterman SJ: Light scattering measurements of the repetitive supersonic implosion of a sonoluminescing bubble. Phys Rev Lett 69:3839–3842, 1992
6. Barnet S: Free radical production: Its biological consequences. Ultrasound Med Biol 24(suppl)29, 1998
7. Bond LJ, Cimino WW: Physics of ultrasonic surgery using tissue fragmentation: II. Ultrasound Med Biol 22:101, 1996
8. Cimino WW, Bond LJ: Physics of ultrasonic energy using tissue fragmentation: I. Ultrasound Med Biol 22:89, 1996
9. Crum L: Sonoluminescence. Phys Today 47:22, 1994
10. Dellius M, Ueberle F, Eisenmenger W: Extracorporeal shock waves act by shock wave-gas bubble interaction. Ultrasound Med Biol 24:1055–1059, 1998
11. Fodor PB, Watson J: Personal experience with ultrasound-assisted lipoplasty: A pilot study comparing ultrasound-assisted lipoplasty with traditional lipoplasty. Plastic Reconstr Surg 101:1103, 1998
12. Gaitan DF, Crum LA, Church CC, et al: Sonoluminescence and bubble dynamics for a single, stable cavitation bubble. J Acoust Soc Am 91:3166–3183, 1992
13. Hiller R, Putterman SJ, Barber BP: Spectrum of synchronous picosecond sonoluminescence. Phys Rev Lett 69:1182–1184, 1992
14. Hiller R, Weninger K, Putterman SJ, et al: Effect of noble gas doping in single bubble sonoluminescence. Science 266:248–250, 1994
15. Holzfuss J, Ruggeberg M, Billo A: Shock wave emissions of a sonoluminescing bubble. Phys Rev Lett 81:5434, 1998
16. Huber P, Jochle K, Debus J: Influence of shock wave pressure amplitude and pulse repetition frequency on the lifespan, size and number of transient cavities in the field of an electromagnetic lithotripter. Phys Med Biol 43:3113–3128, 1998
17. Kandel KB, Harrison LH, McCullough DL: State of

the Art Extracorporeal Shock Wave Lithotripsy. Mount Kisco, NY, Futura, 1987
18. Kenkel JM, Robinson JB Jr, Beran SJ, et al: The tissue effects of ultrasound-assisted lipoplasty. Plastic Reconstr Surg 102:213, 1998
19. Kornfeld M, Suvorov L: On the destructive action of cavitation. J Applied Phys 15:495–506, 1944
20. Landau LD, Lifshitz EM: Fluid Mechanics, ed 2. New York, Pergamon Press, 1987
21. Löfstedt R, Barber BP, Putterman SJ: Toward a hydrodynamic theory of sonoluminescence. Phys Fluids A 5:2911–2928, 1993
22. Masters C, Crane D: The Peroxisome: A Vital Organelle. Cambridge, Cambridge University Press, 1995
23. Matula TJ, Hallaj IM, Cleveland RO, et al: The acoustic emissions from single-bubble sonoluminescence. JASA 103:1377, 1998
24. Miller DL, Thomas RM: The role of cavitation in the induction of cellular DNA damage by ultrasound and lithotripter shock waves in vitro. Ultrasound Med Biol 22:681, 1996
25. Miller DL: Ultrasonic cavitation indirectly induces single strand breaks in DNA of viable cells in vitro by the action of residual hydrogen peroxide. Ultrasound Med Biol 17:729, 1991
26. Nduka CC, et al: Does the ultrasonically activated scalpel release viable airborne cancer cells? Surg Endosc 12:1031, 1998
27. Needham D, Hochmuth RM: Electromechanical permeabilization of lipid vesicles: Role of membrane tension and compressibility. Biophys J 55:1001, 1989
28. Pacifico RI: Ultrasonic energy in phacoemulsification: Mechanical cutting and cavitation. J Cataract Refract Surg 20:338, 1994
29. Prosperetti A: Physics of acoustic cavitation. Rendiconti S.I.F. 93:145–188, 1984
30. Putterman SJ: Sonoluminescence: Sound into light. Sci Am 272:32–37, 1995
31. Putterman S: Sonoluminescence: The star in a jar. Phys World 11:42, 1998
32. Rayleigh L: On the pressure developed in a liquid during the collapse of a spherical cavity. Phil Mag 34:94–98, 1917
33. Reddy JK (ed): Peroxisomes: Biology and role in toxicology and disease. Ann NY Acad Sci, vol 804, 1997
34. Rohrich RJ, Dispaltro FL: Potential long-term effects of ultrasound-assisted lipoplasty: A clinical analysis. Aesthetic Surg J 18:271, 1998
35. Sisto DA, Vijay V, Karmakar M, et al: Use of ultracision harmonic scalpel for isolation or intramyocardial coronary vessels during coronary revascularization of the beating heart. J Thorac Cardiovasc Surg 116:668, 1998
36. Soveral G, Macey RI, Moura TF: Mechanical properties of brush border membrane vesicles from kidney proximal tubule. J Membrane Biol 158:209–217, 1997
37. Svensson B, Mellerio J: Phaco-emulsification causes the formation of cavitation bubbles. Curr Eye Res 13:649, 1994
38. Thomas CR, al-Rubeai M, Zhang Z: Prediction of mechanical damage to animal cells in turbulence. Cytotechnology 15:329–335, 1994
39. Topaz M: Possible long-term complications in ultrasound-assisted lipoplasty induced by sonoluminescence, sonochemistry, and thermal effect. Aesthetic Surg J 18:19, 1998
40. Wanders RJA (ed): Function and biogenesis of peroxisomes in relation to human disease. Amsterdam, Royal Netherlands Academy, 1995
41. Weninger K, Hiller R, Barber BP, et al: Sonoluminescence from single bubbles in nonaqueous liquids: New parameter space for sonochemistry. J Phys Chem 99:14195–14197, 1995
42. Weninger K, Cho H, Hiller R, et al: Sonoluminescence from an isolated bubble on a solid surface. Phys Rev E 56:6745, 1997
43. Weninger K, Barber BP, Putterman S: Pulsed Mie scattering measurements of the collapse of a sonoluminescing bubble. Phys Rev Lett 78:1799–1802, 1997
44. Williams AR, Hughes DE, Nyborg WL: Hemolysis near a transversely oscillating wire. Science 169:871, 1970
45. Williams AR: Effects of ultrasound on blood and the circulation. *In* Nyborg W, Ziskin M (eds): Biological Effects of Ultrasound. New York, Churchill Livingstone, 1985
46. Wu CC, Roberts PH: Shock-wave propagation in a sonoluminescing gas bubble. Phys Rev Lett 70:3424–3427, 1993
47. Zhong P, Cioanta I, Zhu S, et al: Effects of tissue constraint on shock wave-induced bubble expansion in vivo. JASA 104:3126–3129, 1998
48. Zocchi M: Ultrasonic liposculpturing. Aesthetic Plast Surg 16:287, 1992
49. Zocchi M: Ultrasonic assisted lipoplasty. Clin Plast Surg 23:575, 1996
50. Zocchi M: Clinical aspects of ultrasonic liposculpture. Perspect Plast Surg 7:153, 1993

Address reprint requests to

Seth Putterman, PhD
Department of Physics
University of California, Los Angeles
2-234 Knudsen Hall
405 Hilgard Avenue
Los Angeles, CA 90095–1547